Heat Mass Transfer (2015) 51:1–9
DOI 10.1007/s00231-014-1379-0

ORIGINAL

Local nucleation propagation on heat transfer uniformity during subcooled convective boiling

Beom Seok Kim · Gang Mo Yang · Sangwoo Shin · Geehong Choi · Hyung Hee Cho

Received: 25 July 2013 / Accepted: 14 May 2014 / Published online: 29 May 2014
© Springer-Verlag Berlin Heidelberg 2014

Abstract Convective boiling heat transfer is an efficient cooling mechanism to dissipate amount of thermal energy by accompanying the phase transition of the working fluids. Particularly, the amount of heat dissipation capacity can be readily extensible by increasing the degree of subcooling due to initial demands requiring for coolant saturation. Under severely subcooled condition of 60°, we investigate boiling heat transfer phenomena regarding spatial heat transfer uniformity and stability on a planar surface. Severe subcooling can induce locally concentrated thermal loads due to poor spatial uniformity of the heat transfer. For reliable cooling, a high degree of spatial uniformity of the heat transfer should be guaranteed with minimized spatial deviation of heat transfer characteristics. Under pre-requisite safeguards below CHF, we experimentally elucidate the principal factors affecting the spatial uniformity of the heat transfer for a flow/thermal boundary layer considering heat transfer domains from a single-phase regime to a fully-developed boiling regime. Based on the local heat transfer evaluation, we demonstrate that full nucleation boiling over the entire heat transfer surface under subcooling conditions is favorable in terms of the uniformity of heat dissipation through the phase-change of the working fluid.

1 Introduction

In excessive heat-dissipating components and energy-transport systems, thermal stability is essential to achieve reliable heat transfer performance. For example, thermal power-generation systems using fossil fuels or nuclear fission/fusion together with a heat transfer system including boilers and heat exchangers require stable operating conditions with reliable thermal transport characteristics, ensuring the long-term stability and reliability of the system [1–3]. Heat transfer uniformity is one of the critical requirements to ensure that thermally induced failure of components by locally concentrated thermal stresses does not occur [4–6]. As one of the most feasible heat dissipating/transporting methods, convective boiling heat transfer has been applied to such systems using subcooled working fluids to maximize the heat transfer capacity and efficiency.

Boiling heat transfer can be highly efficient to dissipate amount of thermal energy for cooling because of the latent heat associated with the phase-change of the working fluids and the vigorous convection of bubbly flows [7–9]. Particularly, the amount of heat dissipation capacity as well as efficiency can be readily extensible by increasing the degree of subcooling due to initial demands requiring for coolant saturation [10]. Most applications of boiling heat transport, therefore, have been designed with the considerable subcooling of liquid-phase working fluids. However, the severe subcooling can induce locally concentrated thermal loads, because partial nucleation at the transition regions from a single-phase regime to a two-phase regime necessarily involves drastic transitions of fluidic/thermal physics inducing significant spatial temperature gradients even on a small heat transfer area. As an efficient energy transfer mechanism as well as a powerful cooling technique, operating conditions of boiling heat transfer has been designed in a security-domain which does not cause a critical failure of systems by preventing abrupt transitions to film boiling, i.e., ensuring that CHF is not reached [11,

B. S. Kim · G. M. Yang · S. Shin · G. Choi · H. H. Cho (✉)
Department of Mechanical Engineering, Yonsei University, 50 Yonsei-ro, Seodaemun-gu, Seoul 120-749, Korea
e-mail: hhcho@yonsei.ac.kr

12]. Moreover, for reliable heat dissipation performances and robustness in boiling applications with long life-time, heat transfer uniformity must be guaranteed, with a minimal spatial deviation of the heat transfer characteristics. There have been a few novel approaches to enhancing boiling heat transfer performances as well as uniformity via controlling the surface morphology using micro- or nano-scale engineered structures and surface coatings [9, 13–17]. These studies have attempted to elucidate fundamental physics of the heat transfer, relying on structural and interfacial modification to describe the nucleation behavior [17–19]. However, these remain significant problems awaiting solution for their applications to macro-scale thermal systems.

We focus on the local characterization of heat transfer at a planar surface, and attempt to design suitable operating domains for convective boiling heat transfer with the aim of improving heat transfer uniformity in severely subcooled conditions. Under design constraints below CHF, we experimentally elucidate the principal factors on spatial deviations of heat transfer performances of wall superheats and convective heat transfer coefficients (HTCs) regarding flow/thermal boundary layer developments according to heat transfer domains from a single-phase regime to a fully-developed boiling regime. Based on the discussion on the local heat transfer evaluations, we demonstrate that full nucleation boiling over the entire heat transfer surface under subcooling condition is favorable to enhance the uniformity of heat dissipation.

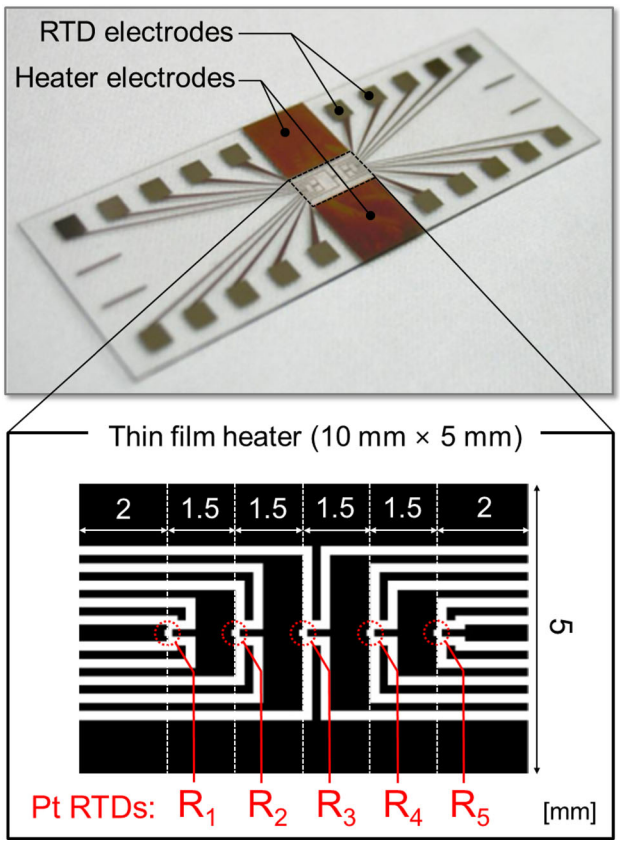

Fig. 1 Local measuring sensor chip with resistance temperature detectors (RTDs) and a thin-film heater. Five RTDs (R_1 to R_5) are arranged in a row just below the heater

2 Materials and methods

2.1 Local measuring sensor and experimental facilities

Figure 1 shows a devised temperature array sensor for local heat transfer characterization. Five four-wire resistance temperature detectors (RTDs) are arranged in a row along the direction of working fluid flow, separated by 1.5 mm. Especially for the accurate local temperature measurements and HTC evaluations, RTDs are located just below a film heater, so that they are able to sense the wall temperature under convective boiling environments. Herein, the sensing area of a single RTD is 120 μm × 120 μm, and the area of the 500-nm-thick film heater is 10 mm × 5 mm. It is necessary for the applied heat flux to be dissipated exclusively via convective heat transfer into the working fluid. Therefore, a thermally insulating Pyrex glass (thermal conductivity of 1.005 W/m K) substrate is employed. Micro-electro-mechanical system (MEMS) techniques are employed in the fabrication process. First, platinum RTDs, which have a reliable linearity of resistance according to temperature variations, are fabricated on the substrate using a metal lift-off process. We use transparent indium tin oxide (ITO) for the film heater, because of its high resistivity apt for electric heating. The ITO film is deposited using sputtering, and Au electrodes are using e-beam deposition and defined using Au lift-off process. An electrical insulation layer, which is composed of a 400-nm/300-nm/400-nm-thick oxide/nitride/oxide multilayer stack grown using plasma-enhanced chemical vapor deposition (PECVD), is formed between the RTDs and the ITO heater.

Figure 2a depicts the experimental facilities used to investigate the convective flow boiling. A 3-kW immersion heater is inserted into a stainless steel reservoir with a capacity of 44 liters to control the temperature of the working fluid, which is deionized water. A pressure gauge and K-type thermocouples are also installed in the reservoir to monitor the conditions of the working fluid. A magnetic pump (TXS5.3, SUS316, Tuthil Co., USA) is used to circulate the working fluid through a closed-loop channel containing a test section, using an electric motor (LG-OTIS, Korea). The closed-loop channel consists of stainless steel pipes wrapped with thermal insulation to reduce thermal losses. A mass-flow meter (Ultramass MK II, Oval Co., Japan) is installed in the flow channel to measure the

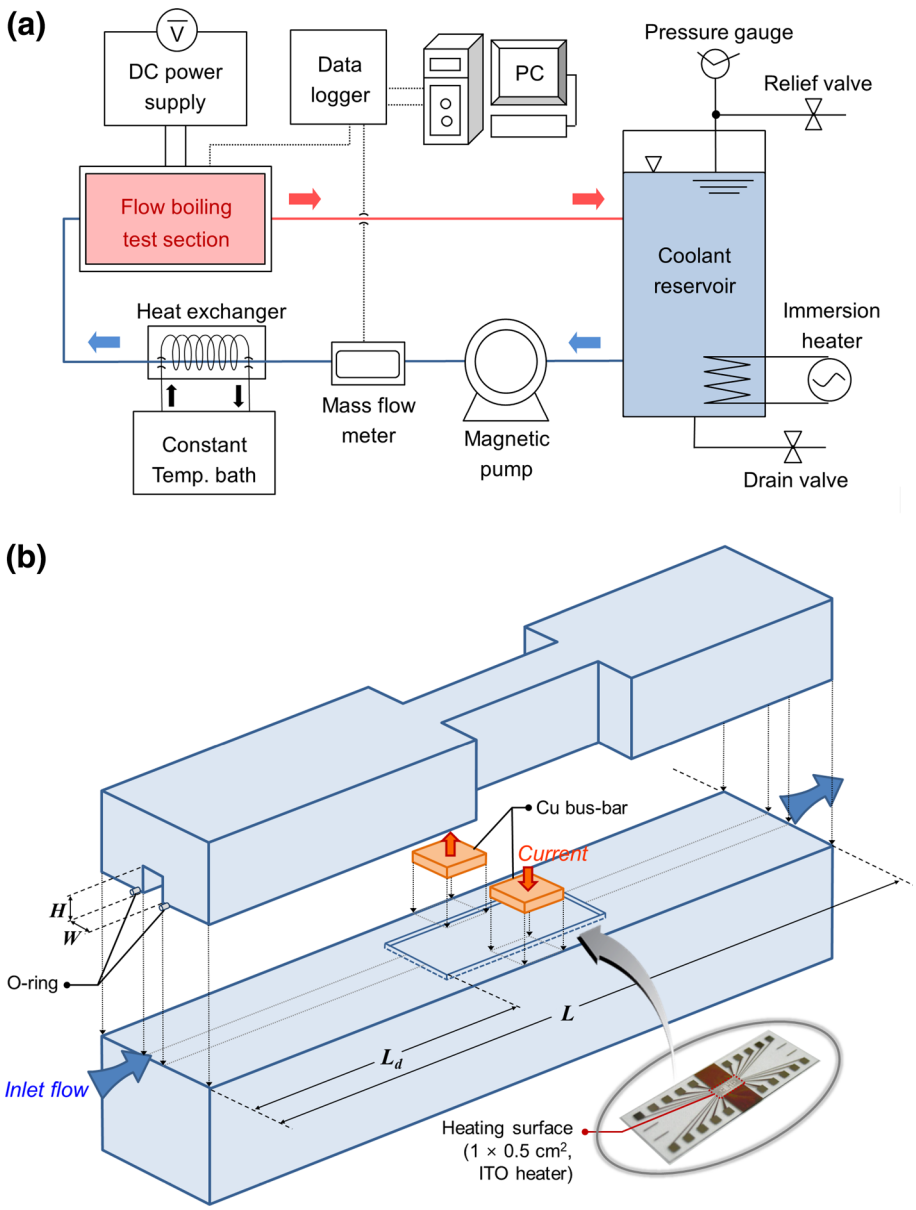

Fig. 2 Experimental apparatus for the evaluation of the convective boiling. **a** Overview of the experimental system with a closed-loop for the working fluid flow and signal monitoring equipment. **b** Test section in a confined flow channel used for the installation of the fabricated sensor chip

flow rate, which can be adjusted by controlling the pump. To accurately regulate the inlet temperature of the working fluid, we use a cross-flow type heat exchanger and a constant temperature bath (42 l–5 kW, Hanil Industrial Machine Co., Korea).

The test section shown in Fig. 2b provides a site to install the fabricated sensor chip in the convective boiling environment. The main body of the test section is assembled from acrylic plastic (thermal conductivity of 0.19 W/m K). The width, W, and the height, H, of the channel are both 8 mm, and the total length of the channel, L, is 375 mm. The distance between the inlet of the channel and the sensor, L_d, is 205 mm, which is more than 25 times of the hydraulic diameter of the channel in order to guarantee fully-developed flow conditions. At the inlet and outlet of the test section, settling chambers are employed to stabilize the working fluid and monitor the temperature and pressures by the K-type thermocouples and pressure gauges. A 2-mm-thick silicone sheet (thermal conductivity of 0.2 W/m K) is located just below the sensor to prevent liquid leakage and reduce conductive heat loss. After the installation of the sensor on the test section, electric circuits are connected via RTDs and the thin film heater on the sensor for acquiring resistance signals and supplying currents, respectively. A DC power supply (200 V-10 A, KSC Korea Switching, Korea) is used to adjust the heat flux through the ITO film heater. Signals from the thermocouples, pressure gauges, RTDs, and the heater in the sensor are acquired by a data logger (34970A, Agilent Technologies, USA) and then processed using a desktop computer.

Prior to commencing the experiments, preconditioning is carried out to remove gases dissolved in deionized-water working fluid by heating it to the saturation point for more than 2 h. Following this, we adjust the inlet temperature of the working fluid to $T_f = 40$ °C to achieve subcooled conditions and a Reynolds number of 4,000 under atmospheric pressure. When the temperature stabilizes at a given heat flux without any monotonic variations, data are acquired during a period of 60 s. We acquire the experimental data at a sample rate of 60 Hz under the steady-state conditions, and then present time-averaged values.

2.2 Analysis on data reduction

For the quantitative evaluation of convective boiling heat transfer, the principal factors on convective boiling heat transfer performances are defined as follows:

2.2.1 Applied heat flux

When an electric current is supplied, the heat flux can be generated by the ITO film heater which is fabricated on the sensor chip. This quantity of thermal load is expressed as follows:

$$q'' = Q/A = (V \times I)/A \tag{1}$$

where Q, A, V and I represent the heat flow rate, area of the heater, voltage drop through the heater and applied electric currents, respectively. The voltage drop is measured between the opposite Au electrodes of the ITO heater, and the electric current is measured using a shunt resistance.

2.2.2 Wall temperature

The local wall temperature is acquired from the RTDs. As a pre-calibration procedure, we validate the linearity of RTDs' resistance according to temperature variations. Each RTD has an independent correlation equation within a temperature range from 300 to 475 K as a linear function of temperature, in the form $T_{w,i} = A_i \cdot \Omega_i + B_i$, where T_w and Ω denote the wall temperature and the electric resistance, respectively. Here A and B are calibration coefficients, and the subscript i is the RTD index. During calibration, we confirm that the calibration should be correlated with sufficient reliability of a statistical coefficient of determination, R^2 higher than 99 %.

2.2.3 Local heat transfer coefficient

The experimental domain covers not only the convective single-phase regime, but also the boiling regime. However, it is difficult to directly quantify boiling heat transfer performances reflecting the detailed physics at the interface because it accompanies vigorous fluidic dynamics with localized phase-changes of the working fluid and convective two-phase flow. Nevertheless, it is possible to denote convective HTCs from the thermal deviation between local hot spots on the solid surface and the convective bulk fluid [16, 20]. As a parameter for representing heat transfer efficiency, the local convective HTCs are evaluated within the entire experimental regime based on the differences between the wall temperature acquired by each RTD and the bulk temperature of the working fluid. This can be expressed based on Newton's law of cooling as follows: [21, 22]

$$h_i = q''/(T_{w,i} - T_f) \tag{2}$$

where h_i and T_f are the local HTC of each RTD and temperature of subcooled working fluid, respectively.

2.3 Uncertainty analysis

We evaluate the reliability of the experimental results based on the Kline's uncertainty analysis [23]. The uncertainties are estimated with a confidence level of 95 % using the acquired data including the temperature and the heat flux. The uncertainty analysis is performed not only for the variables related to the fundamental dimension measurements, but also for the derived quantities of the principal parameters described in the data reduction procedure. The errors in the estimation of the structural dimensions especially for the fabricated sensor are approximately 0.2 %, and those for the temperatures acquired by the thermocouples are ±1.3 K [24]. From the calibration procedure for RTDs on the fabricated chip, the wall temperatures have an uncertainty of 1.1 %. The measured inlet velocity of the convective flow and the Reynolds number have the uncertainty of 1.3 and 2.1 %, respectively. The conductive heat loss through the substrate of the fabricated sensor toward the test section is computed using a commercial computational software package (Fluent 6.3.26, ANSYS). The simulated heat loss could be negligible, owing to the thin geometry of the heater (which is 500-nm-thick) and the thermal insulating characteristics of the Pyrex glass substrate and the acrylic test section with low thermal conductivity of 1.005 W/m K and 0.19 W/m K, respectively. The estimated uncertainty of the applied heat flux, $(\delta q''/q'') = \left[(\delta V/V)^2 + (\delta I/I)^2 + (\delta A/A)^2 + \left(\delta q''_{loss}/q''_{actual}\right)^2\right]^{1/2}$ is 7.3 % based on Eq. (1) considering the heat loss analysis,. The uncertainty of the local HTC, $(\delta h/h) = \left[(\delta q''/\delta q'')^2 + \left(\delta\left(T_w - T_f\right)/(T_w - T_f)\right)^2\right]^{1/2}$ is approximately 7.5 % based on Eq. (2).

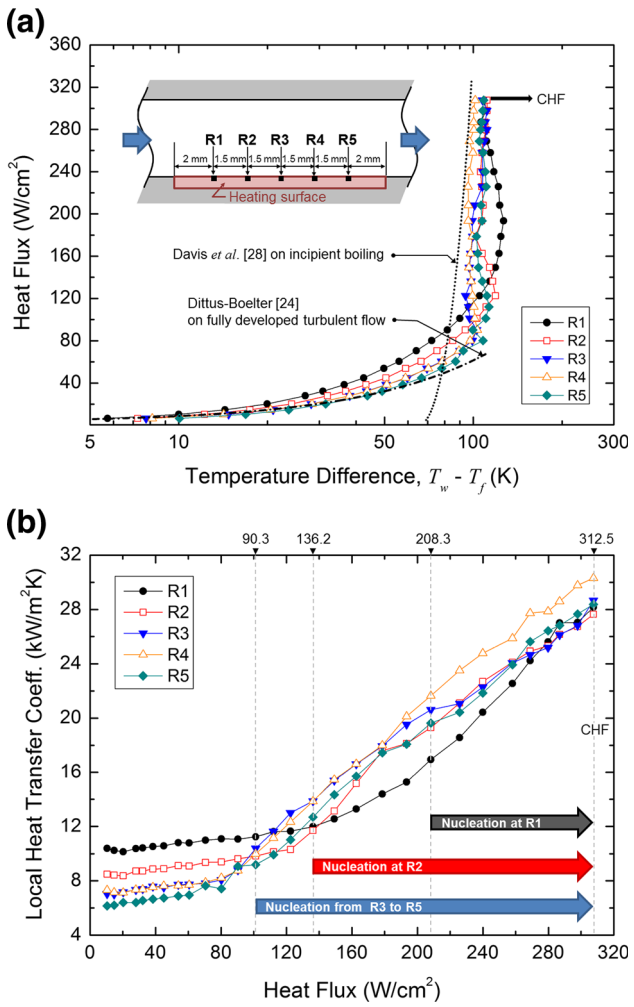

Fig. 3 Local heat transfer performances explaining the transition from single-phase to boiling heat transfer regimes. **a** Boiling *curves* and **b** local heat transfer coefficients evaluated from local measuring sensors of RTDs. The *inset* of (**a**) describes the locations of wall temperature measurement on the sensor chips

3 Results and discussion

From Fig. 3a, the overall heat transfer performances could be clearly classified according to two principal heat transfer mechanisms: subcooled single-phase heat transfer and boiling heat transfer accompanying nucleation of the superheated working fluid [25–27]. In the subcooled single-phase regime, the wall temperature moderately increase according to the increase of applied heat flux. The overall characteristics of single-phase heat transfer are in a good agreement with the well-known correlation for fully developed turbulent flow as follows [28–31]:

$$q''\left(\frac{D_h}{k_f\left(T_w - T_f\right)}\right) = 0.024\mathrm{Re}^{0.8}\mathrm{Pr}_f^{0.4} \tag{3}$$

where q'', D_h, k_f, and Pr_f represent the heat flux, hydraulic diameter of the channel, thermal conductivity of the working fluid, and the Prandtl number of the working fluid, respectively. Following sufficient heating for saturation, incipient boiling can occur. Davis' theoretical equation for the incipient boiling is $q'' = \left[k_l\lambda\rho_v(T_w - T_s)^2\right]/(8\sigma T_s)$ where λ, ρ_v, T_s and σ mean the latent heat of the working fluid, density of the vaporized fluid, saturation temperature and surface tension, respectively [32]. This approximation is valid assuming that surface cavities of all sizes are available for nucleation, and it is also presented in Fig. 3a for reference. Actual partial nucleation during localized onset of nucleation boiling (ONB) occurs at a heat flux of $q''_{ONB} = 90.3$ W/cm^2. In the two-phase flow regime, wall superheats do not have much increase compared with the single-phase heat transfer until a CHF of 312.5 W/cm^2 is reached. From Fig. 3b, it can also be shown that HTCs increase steeply within the two-phase flow regime. These consequences different from the single-phase regime are based on the remarkable enhancement of heat transfer due to vigorous heat dissipation through nucleated bubble generation under convective flow. A principal merit of boiling heat transfer is that the phase-change of the working fluid at the surface, as well as vigorous fluidic behavior accompanying the bubble-induced convective stream, is favorable for heat transport.

Even though the overall heat transfer performances are purely dependent on the typical heat transfer physics, spatial deviations of the characteristics may still result in deterioration of the net heat transfer characteristics in certain flow boiling conditions. We determine that the local temperature distribution and HTCs affect the uniformity of heat transfer in subcooled single-phase flow and nucleation in the boiling regime [33]. From Fig. 3a, b, the local boiling and HTC curves have different heat flux value for a transition from the single-phase to the boiling regime. The subcooled flow significantly affects the upstream region to have less wall superheat and higher HTCs compared to the downstream region within the single-phase regime. Due to the strong subcooling effect, local nucleation consequently occurs at the center of the heating area (i.e., at R_3) and partial nucleation propagates downstream (i.e., towards R_4 and R_5). When the heat flux increases to reinforce the development of a thermal boundary layer for the bubble growth, nucleation sites can propagate upstream against the severe subcooling condition. We found that a heat flux of 208.3 W/cm^2 was required for the boiling regime to fully develop, even though local nucleation started at a heat flux of $q''_{ONB} = 90.3$ W/cm^2. Subcooled convective flow can be a principal reason for spatial non-uniformity of heat transfer due to apparent cooling effects, especially in the upstream region, and a sequential decrease of the heat transfer in the downstream direction due to the development of a thermal boundary layer. These subcooling effects

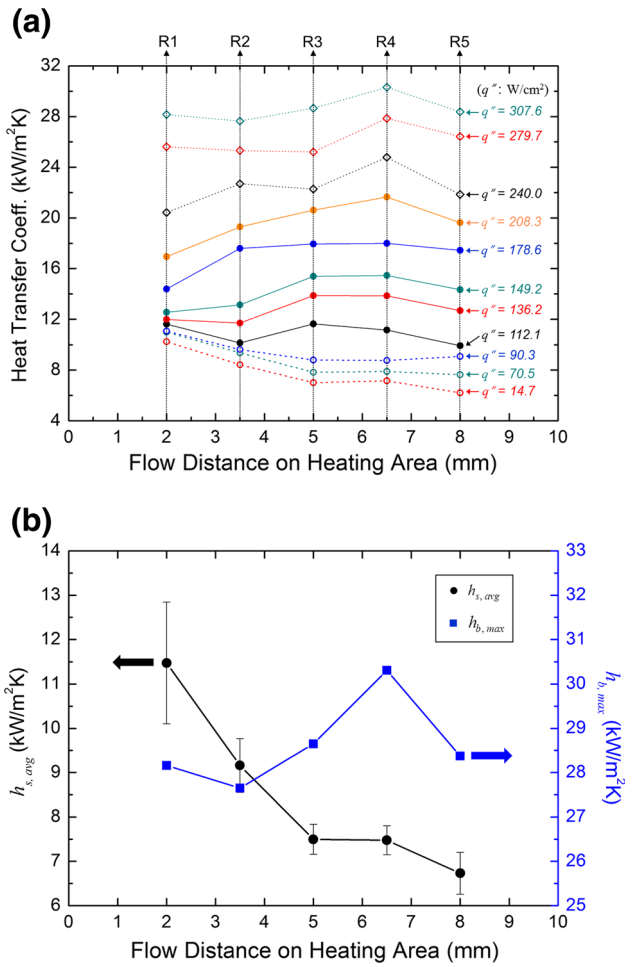

Fig. 4 Local characteristics on convective HTCs. **a** Spatial distribution of HTCs in the flow direction of the working fluid for various applied heat fluxes. **b** Comparison of the spatial distribution of HTC for different heat transfer uniformity; $h_{s,avg}$ is the averaged HTC at each point in the single-phase regime and $h_{b,max}$ is the maximum HTC describing heat dissipation performances at each local point in the boiling regime

on convective heat transfer could dominate the local behavior of a two-phase flow from partial nucleation to the fully-developed boiling regime [27, 34].

Localized variations in the heat transfer of the single-phase and boiling regimes can be inferred from the corresponding fluid and thermal transport characteristics. Figure 4a shows the spatial distribution of HTC according to the increase of applied heat flux. In the single-phase flow regime when the heat flux is less than 90.3 W/cm^2, at first, the subcooled flow stream severely affects the upstream region, and thermal energy is accumulated through the growth of a thermal boundary layer along the flow direction. Therefore, a gradual decrease in the local HTCs can be shown in downstream direction. When partial nucleation is initiated (here, with a heat flux over 90.3 W/cm^2), however, the efficiency of heat dissipation is enhanced significantly, especially on local nucleation sites accompanying bubbly-flow. The increment of HTC from R_3 to R_5, therefore, is exceptional in the nucleate boiling regime over a heat flux range of 112.1–149.2 W/cm^2. As the nucleation sites propagate upstream towards R_2 and R_1 in turn, the overall HTC increases by diminishing spatial HTC deviations. Near CHF condition, a spatial decrease in HTC downstream past R_4 can be shown even though the local HTC continually increases by adding heat flux, and then the most efficient heat transfer is validated at R_4 before the onset of *significant void flow* development [27], which accompanies the fully-development of two-phase bubbly-flow. The bubble-rich stream in the fully-developed region deteriorates heat dissipation due to its thermal-insulating characteristics and disturbance of liquid refreshment. It consequently results in the decrease of heat-dissipating efficiency especially in the downstream accompanying the *significant void flow*.

The averaged and the maximum HTCs at the local points within single-phase and boiling regime are compared to examine the different localized heat dissipating performances with disparate spatial uniformity characteristics. In Fig. 4b, $h_{s,avg}$ and $h_{b,max}$ are defined to represent the averaged heat transfer within single-phase regime and the maximum heat dissipation performance in the nucleate boiling regime at each local point, respectively. These two factors can be expressed as follows:

$$h_{s,avg} \equiv Avg(h_i) \quad \left(0 \le q''_i \le q''_{i,ONB}\right) \tag{4}$$

$$h_{b,\max} \equiv Max(h_i) \quad \left(q''_{i,ONB} \le q''_i \le q''_{i,CHF}\right) \tag{5}$$

From a comparison of the two graphs shown in Fig. 4b, we can explain whether it is in the single-phase or the nucleate boiling regime determines completely different spatial distributions of HTC. At low heat fluxes, subcooled flow dominates the single-phase convective heat transfer, and HTC at R_1 is 53.1 % higher than that at R_3. As the thermal boundary layer develops along the flow direction, HTC decreases because the difference in temperature between the heat transfer surface and the flow stream that is adjacent to it increases. At higher heat fluxes, when boiling heat transfer occurs, the overall heat dissipation significantly increases. Bubble nucleation and rapid detachments are favorable to enhance heat dissipation because of the accompanying phase-change of the working fluid in combination with the turbulent fluidic behavior near the surface. However, bubble nucleation and detachment are hardly shown in the upstream region under the severe subcooling conditions (60 K below the saturation point), and could only be initiated at certain downstream locations if there is sufficient thermal loads to induce a thickening of the thermal boundary layer. As

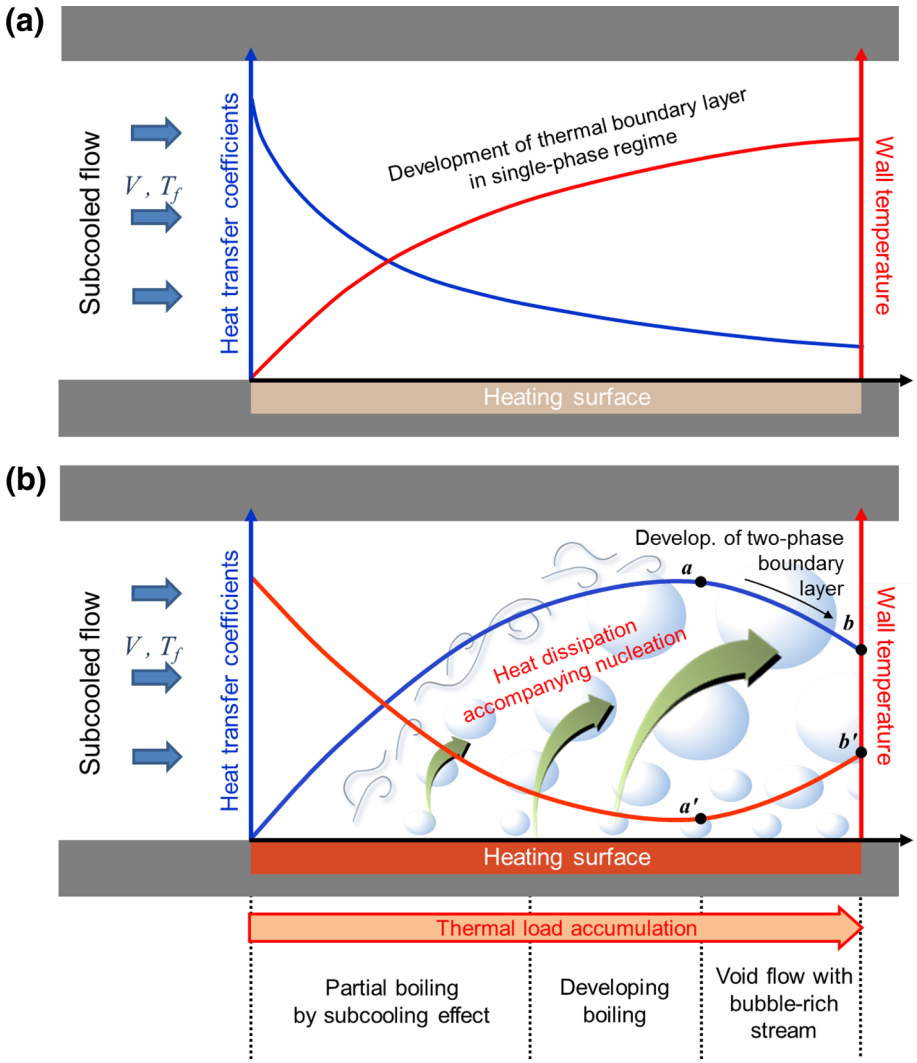

Fig. 5 Schematic diagrams on different characteristics for wall superheat and local HTC, and consequent uniformity in **a** single-phase heat transfer regime and **b** boiling heat transfer regime

the subcooled flow comes to be saturated and developed after the nucleate boiling region near R_4, two-phase bubbly flow develops gradually increasing the vaporized volume in the channel. Therefore, the highest HTC of 30,308 W/m^2 K is obtained at R_4, where vigorous two-phase heat transfer occurs just before the development of significant void flow. Although we are in the fully-developed boiling regime, subcooled flow can still affect especially in the upstream region. From the curve of $h_{b,max}$, HTC in the upstream region of R_1 is slightly higher by 1.9 % compared to R_2, which is located 1.5 mm further downstream. These different characteristics on local HTC and its effect on spatial heat transfer uniformity is schematically illustrated in Fig. 5 regarding the development of significant void flow as well as the subcooling effect. We can conclude that the spatial uniformity of the heat transfer is dependent on the heat transfer regime, i.e., whether we are in the single-phase or boiling domain.

From the previous results on subcooling effects and partial propagation of nucleation, it would be necessary to appreciate that spatial non-uniformity of HTC results in local concentration of thermal loads deteriorating thermal stress. As discussed in Fig. 4b, there is a significant difference of spatial variation in HTCs (by as much as 70.4 % between the first and last sensing points), despite the short length of the heat transfer region which is less than 10 mm long. By combining macro-convective heat transfer with micro-convective boiling physics [35], the minimum spatial deviation of HTCs could be preferable for magnificent heat transfer uniformity. The local heat transfer characteristics reflecting the spatial deviation of HTCs are analyzed in Fig. 6. From Fig. 6a, we can suggest that the propagation of nucleation on the overall heat transfer region can be beneficial to the overall heat transfer characteristics by reducing the spatial non-uniformity of HTCs. Under the single-phase heat transfer in *Region 1*, the effective subcooling and the restricted performance

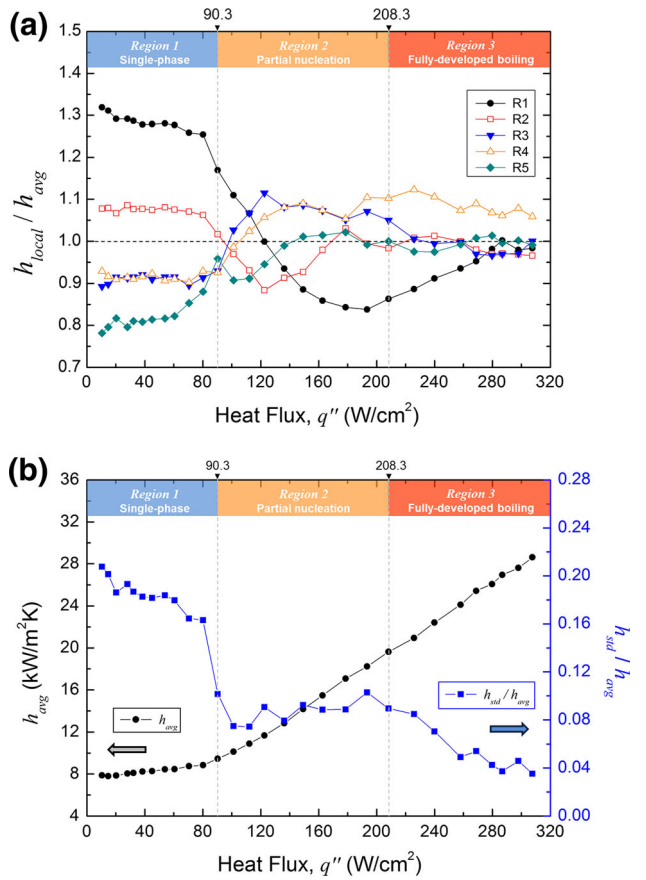

Fig. 6 Local heat transfer characteristics reflecting the behavior of spatial deviation of HTC. **a** Relative variation of local HTCs at each measurement point from R_1 to R_5 compared to the spatially-averaged HTC, h_{avg}, at the same heat flux condition. **b** Variation of the heat transfer uniformity represented by the spatial standard deviation of HTCs normalized by the spatially-averaged HTC

downstream increase the spatial non-uniformity of the local heat transfer with high standard deviations of spatial HTC. The spatial deviation of HTC clearly decreases when the overall heat flux increases, involving a transition from single-phase to two-phase heat dissipation. As nucleate boiling intensifies in *Region 3*, local heat transfer comes to be converged uniformly owing to the propagation of the partial nucleation in the upstream direction all the way across the sensor array. From Fig. 6b, we can find that the spatially averaged HTC, h_{avg} increases with the heat flux, and propagation of partial nucleation upstream remarkably reduces the spatial deviation of HTCs within the transition region, i.e., *Region 2*. After the full nucleation on the entire heat transfer area in *Region 3* when the heat flux exceeds 208.3 W/cm^2, local HTCs come to converge enhancing the spatial uniformity of HTCs and leading to high heat dissipating efficiency. It is a principal merit of severe subcooling condition on convective boiling that it can lead to extended CHF and increase HTC for high capacity and efficiency of heat dissipation, respectively. However, as discussed above, this can cause an amount of spatial deviation of HTCs on a heat transfer surface with significant temperature gradient. We can expect high thermal stresses to occur at a local hot spot, which would result in thermal failure due to the concentration of thermal loads and thermal stress. Based on the consideration of HTC uniformity with regard to the propagation of nucleate boiling, we suggest that full nucleation over the entire heat transfer area is beneficial to mitigating localized concentrations of thermal loads.

4 Conclusions

Subcooling is an important and controllable design factor especially for enhancing heat dissipation performances on flow boiling heat transfer. However, it can deteriorate spatial heat transfer uniformity and stability regarding convective fluidics and vigorous phase-changing behavior. Based on the local heat transfer measurements, we evaluated the spatial distribution of HTCs on a planar heated surface and characterized the principal heat transfer physics regarding flow/thermal boundary layer developments under severe subcooled conditions. We demonstrated that subcooled convective flow can be a principal reason for spatial non-uniformity of heat transfer due to the direct cooling, especially in the upstream region. With the prerequisite domain constraints below CHF, we suggest that full nucleation boiling across the entire heat transfer surface under severe subcooling can resolve concentrated thermal loads by improving the spatial uniformity of heat dissipation through the phase-change of working fluid accompanying vigorous bubbly-flow.

Subcooling effects on convective heat transfer could dominate the local behavior of two-phase flow ranging from partial nucleation to fully-developed boiling, as well as single-phase flow. Severe subcooling (60 K below the saturation temperature) deteriorates non-uniform heat dissipation, with locally concentrated cooling in the upstream region. When fully-developed boiling occurs, even on a small heating area of 10 mm × 5 mm, we have shown that it leads to a significant improvement in the spatial uniformity of the HTCs due to the propagation of nucleation sites across the overall heat transfer surface. Based on the verification of heat transfer uniformity subordinate to convective boiling conditions, we can suggest that further work should be carried out to investigate the necessary conditions for full nucleation across the entire heat transfer surface, in terms of the degree of subcooling and the Reynolds number. In addition, domain control of boiling heat transfer may be more effective by connecting to novel approaches which attempt to control discrete nucleation behavior via micro/nanoscale

engineered surfaces to optimize the uniformity of the heat transfer performances.

Acknowledgments This work was supported by a National Research Foundation of Korea (NRF) Grant funded by the Korea government (MEST) (No. 2011-0017673) and the Human Resources Development program (No. 20134030200200) of the Korea Institute of Energy Technology Evaluation and Planning (KETEP) Grant funded by the Korea government Ministry of Trade, Industry and Energy. The author B. S. Kim is grateful for a Seoul Science Fellowship provided by the Seoul Metropolitan Government.

References

1. Boyd RD (1985) Subcooled flow boiling critical heat flux (CHF) and its application to fusion energy components. Part 1: a review of fundamentals of CHF and related data base. Fusion Technol 7:7–30
2. de Mello FP (1991) Boiler models for system dynamic performance studies. IEEE Trans Power Syst 6:66–74
3. Agostini B, Fabbri M, Park JE, Wojtan L, Thome JR, Michel B (2007) State of the art of high heat flux cooling technologies. Heat Transf Eng 28:258–281
4. Qian G, Nakamura T, Berndt CC (1998) Effects of thermal gradient and residual stresses on thermal barrier coating fracture. Mech Mater 27:91–110
5. Fedorov AG, Viskanta R (2000) Three-dimensional conjugate heat transfer in the microchannel heat sink for electronic packaging. Int J Heat Mass Transf 43:399–415
6. Was GS, Ampornrat P, Gupta G, Teysseyre S, West EA, Allen TR, Sridharan K, Tan L, Chen Y, Ren X, Pister C (2007) Corrosion and stress corrosion cracking in supercritical water. J Nucl Mater 371:176–201
7. Dhir VK (1998) Boiling heat transfer. Annu Rev Fluid Mech 30:365–401
8. Goldstein RJ, Ibele WE, Patankar SV, Simon TW, Kuehn TH, Strykowski PJ, Tamma KK, Heberlein JVR, Davidson JH, Bischof J, Kulacki FA, Kortshagen U, Garrick S, Srinivasan V (2006) Heat transfer—a review of 2003 literature. Int J Heat Mass Transf 49:451–534
9. Li D, Wu GS, Wang W, Wang YD, Liu D, Zhang DC, Chen YF, Peterson GP, Yang R (2012) Enhancing flow boiling heat transfer in microchannels for thermal management with monolithically-integrated silicon nanowires. Nano Lett 12:3385–3390
10. Lucic A, Mayinger F (2010) Transportphenomena in subcooled flow boiling. Heat Mass Transf 46:1159–1166
11. Wu SJ, Shin CH, Kim KM, Cho HH (2007) Single-phase convection and boiling heat transfer: confined single and array-circular impinging jets. Int J Multiph Flow 33:1271–1283
12. Shin CH, Kim KM, Lim SH, Cho HH (2009) Influences of nozzle-plate spacing on boiling heat transfer of confined planar dielectric liquid impinging jet. Int J Heat Mass Transf 52:5293–5301
13. Li C, Wang Z, Wang PI, Peles Y, Koratkar N, Peterson GP (2008) Nanostructured copper interfaces for enhanced boiling. Small 4:1084–1088
14. Chen R, Lu MC, Srinivasan V, Wang Z, Cho HH, Majumdar A (2009) Nanowires for enhanced boiling heat transfer. Nano Lett 9:548–553
15. Kim BS, Shin S, Shin SJ, Kim KM, Cho HH (2011) Control of superhydrophilicity/superhydrophobicity using silicon nanowires via electroless etching method and fluorine carbon coatings. Langmuir 27:10148–10156
16. Kim BS, Shin S, Lee D, Choi G, Lee H, Kim KM, Cho HH (2014) Stable and uniform heat dissipation by nucleate-catalytic nanowires for boiling heat transfer. Int J Heat Mass Transf 70:23–32
17. Betz AR, Xu J, Qiu HH, Attinger D (2010) Do surfaces with mixed hydrophilic and hydrophobic areas enhance pool boiling? Appl Phys Lett 97:141909
18. Patankar NA (2010) Supernucleating surfaces for nucleate boiling and dropwise condensation heat transfer. Soft Matter 6:1613–1620
19. Stephan P, Fuchs T (2009) Local heat flow and temperature fluctuations in wall and fluid in nucleate boiling systems. Heat Mass Transf 45:919–928
20. Khanikar V, Mudawar I, Fisher T (2009) Effects of carbon nanotube coating on flow boiling in a micro-channel. Int J Heat Mass Transf 52:3805–3817
21. Mills AF (1999) Basic heat and mass transfer, 2nd edn. Prentice Hall, Upper Saddle River
22. Incropera FP (2007) Fundamentals of heat and mass transfer, 6th edn. Wiley, Hoboken
23. Kline SJ (1985) The purposes of uncertainty analysis. J Fluids Eng 107:153–160
24. Kim BS (2011) Boiling heat transfer enhancement by micro-nanoscale surface manipulation. Dissertation, Yonsei University
25. Bergles AE, Rosenow WM (1964) The determination of forced-convection surface-boiling heat transfer. J Heat Transf Trans ASME 86:365–372
26. Sato T, Matsumura H (1964) On the conditions of incipient subcooled-boiling with forced convection. Bull JSME 7:392–398
27. Kandlikar SG (1998) Heat transfer characteristics in partial boiling, fully developed boiling, and significant void flow regions of subcooled flow boiling. J Heat Transf Trans ASME 120:395–401
28. Dittus FW, Boelter LMK (1985) Heat transfer in automobile radiators of the tubular type. Int Commun Heat Mass Transf 12:3–22
29. Hino R, Ueda T (1985) Studies on heat transfer and flow characteristics in subcooled flow boiling—Part 1. Boiling characteristics. Int J Multiph Flow 11:269–281
30. Kakaç S, Shah RK, Aung W (1987) Handbook of single-phase convective heat transfer. Wiley, New York
31. Carey VP (2008) Liquid-vapor phase-change phenomena: an introduction to the thermophysics of vaporization and condensation processes in heat transfer equipment, 2nd edn. Taylor and Francis, New York
32. Davis EJ, Anderson GH (1966) The incipience of nucleate boiling in forced convection flow. AIChE J 12:774–780
33. Basu N, Warrier GR, Dhir VK (2002) Onset of nucleate boiling and active nucleation site density during subcooled flow boiling. J Heat Transf Trans ASME 124:717–728
34. Steiner H, Kobor A, Gebhard L (2005) A wall heat transfer model for subcooled boiling flow. Int J Heat Mass Transf 48:4161–4173
35. Chen JC (1966) Correlation for Boiling Heat Transfer to Saturated Fluids in Convective Flow. Ind Eng Chem Process Des Dev 5:322–329